Magneto-mechanically coupled electromagnetic harvesters for broadband energy harvesting

P. V. Malaji, and S. F. Ali

Citation: Appl. Phys. Lett. **111**, 083901 (2017); doi: 10.1063/1.4997297
View online: http://dx.doi.org/10.1063/1.4997297
View Table of Contents: http://aip.scitation.org/toc/apl/111/8
Published by the American Institute of Physics

Magneto-mechanically coupled electromagnetic harvesters for broadband energy harvesting

P. V. Malaji[a] and S. F. Ali[b]
Department of Applied Mechanics, IIT–Madras, Chennai 600 036, India

(Received 30 March 2017; accepted 20 July 2017; published online 25 August 2017)

A low frequency magneto-mechanically coupled energy harvesting system is proposed to increase the power magnitude and bandwidth simultaneously. The system consists of two pendulums that are magnetically and mechanically coupled. The analytical formulation for the coupled system is developed based on the extended Lagrangian formulation. The experimental and simulated results are reported. The results exhibiting the benefits of magneto-mechanical coupling are reported. The experiments show an increment of 30.69% in the power magnitude and 100% enhancement in the bandwidth when compared to independent harvesters even at a low amplitude of excitation. Moreover, Chaos is observed at low frequency and at a low amplitude, which tends to provide larger bandwidths with more power. *Published by AIP Publishing.*
[http://dx.doi.org/10.1063/1.4997297]

Vibration energy harvesting has attracted numerous researchers as a promising solution to make self-sustained, lower-powered electronic devices.[1,2] It can convert energy from vibrating sources into useful electric forms, especially when it is vibrating near/at the host natural frequency. The harvested energy can be used in many disciplines including medical, biology, mechanical, civil infrastructure, and also in computer science.[2] Generally speaking, the energy harvesting field has a significant effect on the improvement of end user's daily life in our society. Conventional linear harvesters are efficient at resonance, which limits their prospects under broadband excitations or in uncertain environments.[3,4] Currently, harvesters are designed with larger bandwidth (BW) or with frequency tuning mechanisms to accommodate uncertain natural frequencies and broadband excitations.

Various passive[5] and active[6] techniques are adopted to adaptively tune to host resonating frequency. Approaches reported are resonance shifts using magnetic methods to modify electromechanical stiffness.[5] Adaptive tuning is useful when excitation is narrow band and unknown. It fails to provide efficient harvesting under random excitations or excitations with broader bandwidths. Furthermore, many tuning mechanisms require an external power source.[6]

Multiple harvesters are often used to scavenge power at multiple frequencies and under broadband excitations.[7,8] Harvesters with similar parameters are attached together and tuned to a single frequency to generate more power at the known frequency. Multiple mistuned harvesters are often used to harvest wideband power but with reduced magnitude of power.[9,10] Nonlinearity in the mechanical design is also exploited to obtain broadband nature of harvesters. An inverted beam with tip mass exploiting buckling induced instability was reported for bandwidth scavenging.[11,12] Nonlinearity due to magnetic interactions has also been reported widely. A Moon's beam under the magnetic field has shown potential for broadband harvesting.[13–15] Other techniques to harvest broadband power include magnetic interactions in 3*D* physical space,[16] exploitation of internal resonance,[17] magnetic coupling between cantilever beams,[18,19] etc., to name a few.

Studies in the literature have reported either enhancement in bandwidths or increase in power using a multiple harvester design. Harvesters that increase power as well as enhance bandwidths are less reported.[20] This letter reports both the enhancement in the operating bandwidth and the increase in scavenged power within that bandwidth, using magneto-mechanically coupled harvesters.[21] The idea is to use multiple scavengers with mistuned parameters and then couple mechanically to increase power magnitude. Under the magnetic field, they generate power at broader bandwidths. This letter reports both magnetic and mechanical coupling (MmCH) at one place.

This letter presents low frequency (<5 Hz) magneto-mechanically coupled electromagnetic harvesters subjected to low amplitude excitation. The system consisting of two pendulum harvesters (uses electromagnetic transductions) exploits chaos at low frequency and at low amplitude to harvest power. Harvesters are chosen such that they have different natural frequencies. Pendulums are pivoted at one end and magnets at the other end as shown in Fig. 1(a). Copper coils are placed beside each magnet for electromagnetic energy generation. The natural frequency of the system can be adjusted changing the stiffness of springs k_1, k_2, and k_3. The springs are attached at a distance a from the pivot. Mechanical coupling (mCH) between pendulums is represented by a spring k_2. The dynamics of the system due to magneto-mechanical coupling is different from that introduced due to the spring hardening and softening as reported by Mann and Sims.[22]

The prototype of the proposed harvester and its experimental setup are shown in Fig. 1(b). The prototype consists of two aluminium pendulums pivoted and magnets attached at the other end. Copper coils are placed beside each magnet. Springs are attached at 20 mm from the pivot. Parameters used for numerical simulation and experimental work are reported in Table I. Pendulums are kept at a distance of

[a]Electronic mail: pradeepmalaji@gmail.com
[b]Electronic mail: sfali@iitm.ac.in

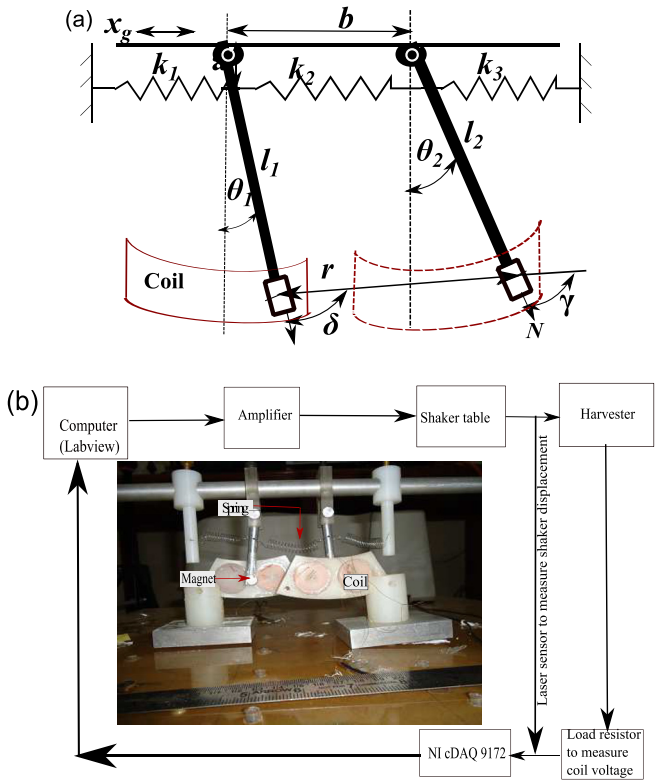

FIG. 1. (a) Schematic of a magneto-mechanically coupled harvesting system and (b) block diagram of the experimental setup.

$b = 55$ mm for magnetic interactions. A load resistance of 160 Ω (equal to measured coil resistance) is used to obtain optimal power.

The system dynamics is developed using the Lagrange equation,[23–25] which in its general form is given as

$$\frac{d}{dt}\left(\frac{\partial \mathcal{L}}{\partial \dot{\theta}_i}\right) - \frac{\partial \mathcal{L}}{\partial \theta_i} = \frac{\partial D}{\partial \dot{\theta}_i}, \tag{1}$$

where $i = 1$, 2, and the Lagrangian ($\mathcal{L}$) is given by $\mathcal{L} = T - \Pi$. The expression in RHS is due to the energy loss in the system.

The kinetic energy (T) of the system is given as

$$T = \frac{1}{2}m_1\left(\frac{(l_1\dot{\theta}_1)^2}{3} + \dot{x_g}^2 + \dot{x}_g\dot{\theta}_1 l_1\cos\theta_1\right) + \frac{1}{2}m_2\left(\frac{(l_2\dot{\theta}_2)^2}{3} + \dot{x_g}^2 + \dot{x}_g\dot{\theta}_2 l_2\cos\theta_2\right). \tag{2}$$

The total potential energy (Π, due to mechanical and magnetic coupling) of the system is given as

$$\Pi = m_1 g\frac{l_1}{2}(1-\cos\theta_1) + \frac{k_1}{2}(a\sin\theta_1)^2 + \frac{k_2}{2}(a\sin\theta_1 - a\sin\theta_2)^2 + \frac{k_3}{2}(a\sin\theta_2)^2 + m_2 g\frac{l_2}{2}(1-\cos\theta_2) + \Pi_m, \tag{3}$$

where Π_m is the magnetic potential between harvesters and is given by[26]

$$\Pi_m(\hat{\boldsymbol{m}}_1, \hat{\boldsymbol{m}}_2, r) = 1/4\,\frac{\mu_0\,(\hat{\boldsymbol{m}}_1\hat{\boldsymbol{m}}_2 - 3\,(\hat{\boldsymbol{m}}_1\bar{\boldsymbol{n}})(\hat{\boldsymbol{m}}_2\bar{\boldsymbol{n}}))}{\pi\, r^3}, \tag{4}$$

where $\bar{\boldsymbol{n}} = \boldsymbol{r}/r$ is the unit vector along the line joining magnets and $r = |\boldsymbol{r}|$. $\hat{\boldsymbol{m}}_1$ and $\hat{\boldsymbol{m}}_2$ are the magnetic dipole moments, b is the distance between the pendulum pivots, and θ_1 and θ_2 are the relative angular displacement of the pendulums.

The magnitude of the distance between magnetic dipoles r is given as

$$r = \sqrt{(b + l_2\sin(\theta_2) - l_1\sin(\theta_1))^2 + (l_2\cos(\theta_2) - l_1\cos(\theta_1))^2}. \tag{5}$$

Magnetic dipole moment $\hat{m} = |\hat{\boldsymbol{m}}|$ in terms of residual magnetic flux B_r, volume of magnet $\hat{V}$, and magnetic constant ($\mu_0 = 4\pi 10^{-7}$ H/m) is given as

$$\hat{m} = \frac{B_r}{\mu_0}\hat{V}. \tag{6}$$

Substituting expressions from (5) and (6) in (4), magnetic potential in terms of angular displacement is given as

$$\Pi_m(\theta_1, \theta_2) = 1/4\,\frac{\mu_0\,(\hat{m}_1\hat{m}_2\cos(-\theta_2 + \theta_1) - 3\,\hat{m}_1\hat{m}_2\cos(\delta)\cos(\gamma))}{\pi\, r^3}, \tag{7}$$

where δ and γ are the angles between the dipole axis and the line joining dipole axis. δ and γ are the functions of θ_1 and θ_2. RHS of (9) is due to the energy loss in the system due to damping and is given by the following expression:

$$D = \frac{1}{2}(c_m + c_e)l_1^2\dot{\theta}_1^{\,2} + \frac{1}{2}(c_m + c_e)l_2^2\dot{\theta}_2^{\,2} \tag{8}$$

with c_m and c_e being the mechanical and electrical damping, respectively.

Substituting (2), (3), and (8) in (1), we get the following equations of motion:

$$\begin{aligned} &I_1\ddot{\theta}_1 + (c_m + c_e)l_1^2\dot{\theta}_1 + m_1 g\frac{l_1}{2}\sin\theta_1 + k_1a^2(\sin\theta_1)\cos\theta_1 \\ &\quad + k_2a^2(\sin\theta_1 - \sin\theta_2)\cos\theta_1 + M_{m1} = -m_1 l_1\ddot{x}_g\cos\theta_1, \\ &I_2\ddot{\theta}_2 + (c_m + c_e)l_2^2\dot{\theta}_2 + m_2 g\frac{l_2}{2}\sin\theta_2 + k_3a^2(\sin\theta_2)\cos\theta_2 \\ &\quad + k_2a^2(\sin\theta_2 - \sin\theta_1)\cos\theta_2 + M_{m2} = -m_2 l_2\ddot{x}_g\cos\theta_2. \end{aligned} \tag{9}$$

Harmonic support excitation, $x_g = X\sin(\omega t)$, has an amplitude X and frequency ω. For magnets under repulsion,

TABLE I. Parameter values considered in the study.

$c_m = 0.004$ Ns/m	$c_e = 0.002$ Ns/m
$l_1 = 60$ mm	$l_2 = 60$ mm
$m_1 = 13$ g	$m_2 = 13$ g
$B_r = 0.6$ T	$k_1 = 8$ N/m
$k_2 = 1$ N/m	$k_3 = 4$ N/m

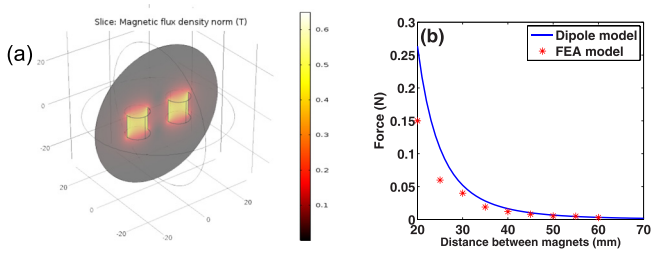

FIG. 2. Validity of magnetic dipole assumption, (a) finite element (FE) model of magnets with magnetic flux density distribution and (b) comparison between FE simulation and analytical results. FE simulation is carried out using Comsol Multiphysics.

$M_{m1} = \frac{\partial \Pi_m}{\partial \theta_1}$ and $M_{m2} = \frac{\partial \Pi_m}{\partial \theta_2}$. Voltage induced due to electromagnetic induction in the coil of length L, resistance R, and surface magnetic flux density B_s is given as $v_i = B_s L l_i \dot{\theta}_i$. Power harvested across load resistance R_L is calculated as $P_i = v_i^2/(R_L + R)$.

The equations developed here are based on magnetic dipole assumption, whereas the magnets used in the experiments have physical dimensions. To validate the assumption made here, a finite element simulation is carried out using COMSOL Multiphysics®. Magnetic interactions are simulated using 3–*D* models as shown in Fig. 2(a). Cylindrical magnets of radius 5 mm, thickness 10 mm, and magnetization 477.46 kA/m are used for simulation. Analytical interactions using dipoles are separately carried out and compared. Figure 2(b) shows that when the magnets are closer, the dipole theory deviates from the simulation. A distance of 40 mm and above provides reasonable accuracy using the dipole assumption. For analytical, numerical, and experimental studies reported in this letter, a nominal separation of 55 mm is considered. This is to avoid the close interaction between magnets below 40 mm during the motion.[22,27]

Upward (forward) and downward (backward) frequency sweeps are carried out in simulations and experiments for a frequency range of 2–4 Hz since the harvester is designed for low frequencies. The amplitude of excitation is kept constant at 2.3 mm.

Figure 3 shows frequency response curves of power harvested for independent harvesters (IH, no magnetic interaction and $k_2 = 0$) and magnetically coupled harvesters (MCH). The qualitative match between simulated and experimental results is observed. However, quantitative discrepancies that exist could be due to the difference in damping values. The IH system with natural frequencies of 2.85 Hz and 3.24 Hz shows weak nonlinearity with a slight shift towards the left. For a higher excitation level with larger oscillations, a strong nonlinear response may be expected.[21] For the MCH system, the nonlinearity is quite evident from the responses. Pendulum-2 in MCH produces slightly more power (230 μW) than that in IH (200 μW). The bandwidth in MCH is 0.9 Hz, which is 150% more than that in IH (0.3 Hz) at a power level of 70 μW. The bandwidth is calculated as the range of frequencies at which the harvester scavenges a constant power. This letter takes an example of 70 μW. This improvement in pendulum-2 performance can be attributed to magnetic coupling between pendulums. Pendulum-1 produces lower power in MCH (91 μW) compared to the IH (265 μW). During frequency sweep between two near resonances of the system,

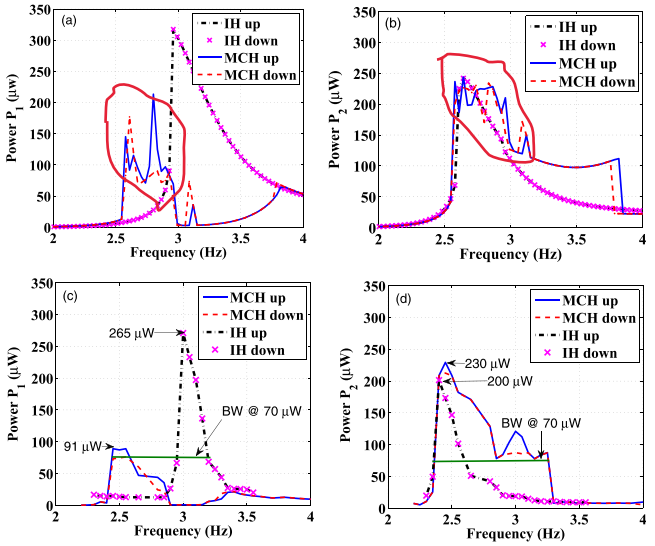

FIG. 3. Power curves with/without magnetic coupling, (a) and (b) simulated results and (c) and (d) experimental results. Bandwidth (BW) at 70 μW, for P_1 (IH: 2.95–3.23 Hz, MCH: 2.45–2.65 Hz) and for P_2 (IH: 2.35–3.65 Hz, MCH: 2.35–3.25 Hz) with P_1: pendulum-1 and P_2: pendulum-2.

energy shifts from one pendulum to the other. Hence, a decrease in the bandwidth of (0.2 Hz) 28% compared to the IH (0.28 Hz) at 70 μW is observed. In such cases, one acts as an auxiliary oscillator for the other pendulum (pendulum-2) as described by Tang and Wang.[20]

Mechanical coupling (mCH) between pendulums shifts the natural frequencies to 2.93 Hz and 3.35 Hz. It also reduces the power harvested by pendulum-1 as shown in Fig. 4(c) (192 μW) compared to the IH [265 μW, see Fig. 3(c)]. The magnitude of power harvested by pendulum-2 in mCH increases (from 240 μW to 255 μW) as compared to IH [refer Figs. 3(d) and 4(d)].

With both magnetic and mechanical (MmCH) coupling, the bandwidth of pendulum-1 in upward sweep at 70 μW is 0.5 Hz, which is 66.6% more than that obtained by mCH

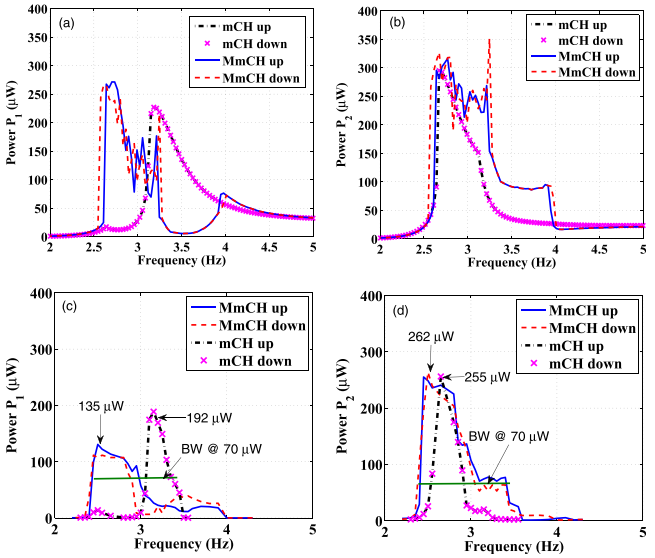

FIG. 4. Response curves with magneto-mechanical coupling: (a) and (b) simulated power curves and (c) and (d) experimental power curves. Bandwidth (BW) at 70 μW, for P_1 (mCH: 3.1–3.4 Hz, MmCH: 2.5–3 Hz) and for P_2 (mCH 2.55–2.9 Hz, MmCH 2.35–3.45 Hz).

(0.3 Hz) as shown in Fig. 4(c). The reduction in power from 192 μW (mCH) to 135 μW (MmCH) is also observed as expected. The power magnitude of pendulum-2 increases slightly for MmCH (262 μW) compared to mCH (255 μW), whereas a 162% increase in the bandwidth compared to mCH (0.35 Hz to 1.1 Hz) at 70 μW during the forward sweep is observed [refer Fig. 4(d)].

Magnetic coupling alone broadens the operating bandwidth, but magneto-mechanical coupling is observed to increase both the bandwidth and the power scavenged. The bandwidth of pendulum-1 at 70 μW increases by 150% (0.2 Hz–0.5 Hz) for MmCH compared to MCH [please refer Figs. 3(c) and 4(c)] along with the increase in power magnitude from 91 μW to 136 μW. The bandwidth of pendulum-2 increases by 22% (0.9 Hz–1.1 Hz) at 70 μW, and the power scavenged increases from 233 μW to 251 μW. This proposed MmCH provides wider bandwidths compared to MCH, mCH, and IH.

The presence of nonlinearity and chaos is evident from Fig. 5, which shows simulated responses of pendulum-2 in MmCH. The phase plots show a route to chaos. A transition occurs from high voltage chaos at 2.65 Hz in Fig. 5(a) to a low voltage periodic oscillation shown at Fig. 5(c). The chaotic response of the pendulum can be attributed to geometric nonlinearity induced due to magnetic coupling. Similar trends are observed for pendulum-1. Figure 5(d) shows the bifurcation diagram for pendulum 1. Chaos exists within a frequency band and then again the response becomes periodic at higher frequencies. If designed to operate within the frequency bandwidth, the magneto-mechanical system can harvest more power. In the absence of magnetic coupling, large amplitude oscillations will not induce any chaotic response.[28]

The total power of the system is obtained by summing power harvested from each of the pendulums as shown in Fig. 6. Figure 6(a) shows the power curve for MCH and IH. The maximum power magnitude increases from 290 μW to 318 μW with magnetic coupling. MCH also produces a

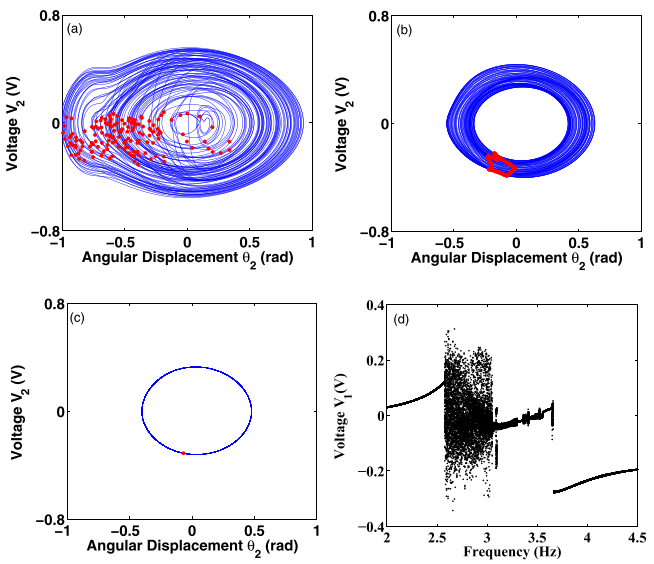

FIG. 5. Simulated phase orbit and Poincare map showing route to chaos of pendulum-2 (a) at 2.65 Hz, (b) at 3.15 Hz, and (c) at 3.3 Hz. (d) The bifurcation diagrams of the voltage output as a function of frequency.

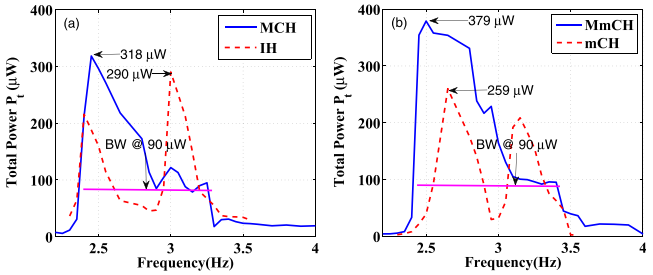

FIG. 6. Total power obtained experimentally. (a) MCH and IH and (b) MmCH and mCH.

continuous bandwidth of 0.9 Hz (2.35 Hz–3.25 Hz) at 90 μW, whereas IH has a split bandwidth of 0.55 Hz (2.35 Hz–2.65 Hz and 2.95 Hz–3.2 Hz). The MmCH system dominates in both the power magnitude and bandwidth. MmCH produces a power of 379 μW compared to 259 μW for mCH [see Fig. 6(b)]. A continuous bandwidth of 1.1 Hz (2.35 Hz–3.45 Hz) is obtained at a power magnitude of 90 μW compared to a split bandwidth of 0.7 Hz (2.55–2.9 Hz and 3.05 Hz–3.4 Hz) as in the case of mCH.

The difference in experimental and simulated results can be attributed to slight bending of the springs connected to pendulums during experiments in addition to deviation in damping. In general, qualitative match between simulation and experimental results is observed.

In summary, this letter explores magneto-mechanically coupled harvesters which work at low frequency and low amplitude. It shows a route to chaos at very low frequency and harvest larger power with that frequency band. The designed prototype has shown promise and harvests 19.1% more power (318–379 μW) and has 22.2% more bandwidth (0.9–1.1 Hz) than the only magnetically coupled system, whereas in comparison to independent harvesters, an increment of 30.69% in power magnitude and 100% in frequency bandwidth is obtained.

The authors are thankful to the Department of Science and Technology, India for funding the research work (Project No. DST-YSS/2014/000336).

[1]C. Williams and R. Yates, in *Proceedings of the International Solid-State Sensors and Actuators Conference—TRANSDUCERS'95* (1995), Vol. 1, p. 8.
[2]J. A. Paradiso and T. Starner, IEEE Pervasive Comput. **4**, 18 (2005).
[3]S. Roundy and P. K. Wright, Smart Mater. Struct. **13**, 1131 (2004).
[4]S. F. Ali, M. I. Friswell, and S. Adhikari, Smart Mater. Struct. **19**, 1 (2010).
[5]V. R. Challa, M. G. Prasad, Y. Shi, and F. T. Fisher, Smart Mater. Struct. **17**, 1 (2008).
[6]S. Roundy and Y. Zhang, Proc. SPIE **5649**, 373–384 (2005).
[7]Q. Ou, X. Chen, S. Gutschmidt, A. Wood, N. Leigh, and A. F. Arrieta, J. Intell. Mater. Syst. Struct. **23**, 117 (2012).
[8]L. J. Gong, Q. S. Pan, W. Li, G. Y. Yan, Y. B. Liu, and Z. H. Feng, Appl. Phys. Lett. **107**, 231110 (2015).
[9]P. Malaji and S. F. Ali, Sens. Actuators A **255**, 1 (2017).
[10]I. Sari, T. Balkan, and H. Kulah, Sens. Actuators, A **145–146**, 405 (2008).
[11]M. I. Friswell, S. F. Ali, O. Bilgen, S. Adhikari, A. W. Lees, and G. Litak, J. Intell. Mater. Syst. Struct. **23**, 1505 (2012).
[12]C. Lan, W. Qin, and W. Deng, Appl. Phys. Lett. **107**, 093902 (2015).
[13]A. Erturk, J. Hoffmann, and D. J. Inman, Appl. Phys. Lett. **94**, 254102 (2009).
[14]S. F. Ali, S. Adhikari, M. I. Friswell, and S. Narayanan, J. Appl. Phys. **109**, 074904 (2011).

[15]K. A. Kumar, S. F. Ali, and A. Arockiarajan, J. Sound Vib. **393**, 265 (2017).
[16]H. Wang, F. Hu, K. Wang, Y. Liu, and W. Zhao, Appl. Phys. Lett. **110**, 163905 (2017).
[17]L. Xiong, L. Tang, and B. R. Mace, Appl. Phys. Lett. **108**, 203901 (2016).
[18]W. J. Su and W. Z. Jean, J. Intell. Mater. Syst. Struct. **25**, 1 (2013).
[19]S. Zhou, J. Cao, W. Wang, S. Liu, and J. Lin, Smart Mater. Struct. **24**, 1 (2015).
[20]L. Tang and Y. Yang, Appl. Phys. Lett. **101**, 094102 (2012).
[21]P. V. Malaji and S. F. Ali, in *2016 IEEE 1st International Conference on Power Electronics, Intelligent Control & Energy Systems (ICPEICES)* (2016), pp. 1–5.
[22]B. Mann and N. Sims, J. Sound Vib. **319**, 515 (2009).
[23]W. T. Thomson, *Theory of Vibration* (CBS, 2002).
[24]H. Goldstein, C. Poole, and J. Safko, *Clasical Mechanics* (Addison Wesley, 2000).
[25]B. P. Mann, J. Sound Vib. **323**, 864 (2009).
[26]K. W. Yung, P. B. Landecker, and D. D. Villani, Magn. Electr. Sep. **9**, 39 (1998).
[27]D. Upadrashta, Y. Yang, and L. Tang, J. Intell. Mater. Syst. Struct. **26**, 1980 (2015).
[28]P. V. Malaji and S. F. Ali, Eur. Phys. J. Spec. Top. **224**, 2823 (2015).